

Semiconductor quantum dot resonant tunnelling spectroscopy

Mark A Reed†, John N Randall‡ and James H Luscombe‡

†Yale University, New Haven, CT 06520, USA

‡Central Research Laboratories, Texas Instruments Incorporated, Dallas, TX 75265, USA

Abstract. Recently, three-dimensionally laterally confined semiconductor quantum wells ('quantum dots') have been realized. These structures are analogous to semiconductor atoms, with energy level separation of order 25 meV, and tunable by means of the confining potentials. A systematic study reveals a (radius)⁻¹ dependence on the energy separation. The electronic transport through quantum dots is presented and analysed. The spectra correspond to resonant tunnelling from laterally confined emitter contact subbands through the discrete three-dimensionally confined quantum dot states. The effects of two dots in series, and Fermi level effects, are presented.

1. Introduction

The creation of 0D electronic systems ('quantum dots') [1–7] is intriguing since these structures are analogous to semiconductor atoms, with energy levels tunable by means of the confining potentials. A configuration for the lateral confinement of a heteroepitaxial resonant tunnelling structure is adopted, where the quasi-bound momentum component (and thus the resultant transport direction) is epitaxially defined in the form of a resonant tunnelling structure, and additional confinement is fabrication-imposed. This configuration is distinct in that the current flow is through, not along, the interface. Tunnelling spectroscopy then probes the low-dimensional states. Because of this configuration, the behaviour of a system operated far from equilibrium can be examined.

2. 1D–0D tunnelling

The fabrication of these structures has been previously reported [1, 2]. The approach essentially embeds a quasi-bound quantum dot between two quantum wire contacts. Creation of dots smaller than 500 Å is possible, though we will show that the appropriate range for the typical epitaxial structure and process used is in the range 1000 Å–2500 Å in diameter. A SEM of a collection of these etched structures is seen in figure 1. Contact is made to just a single structure, so the resulting transport is tunnelling spectroscopy of a single dot.

This experimental embodiment has been previously reported. The current–voltage–temperature characteristics of these structures typically exhibit a clear series of additional NDR peaks at low temperatures, as shown in figure 2. Variation of the lateral diameter by more than

one order of magnitude verifies an approximate R^{-1} energy splitting dependence, indicating energy quantization by the lateral potential instead of single-electron charging, which would have an R^{-2} dependence [8].

We have used a full 3D zero-current, finite-temperature Thomas–Fermi screening model to obtain the energies of the 1D emitter (and collector) and 0D quantum dot states under arbitrary applied bias [2]. Figure 3 shows the crossings of the emitter subband level (n') with the quantum dot levels (n) as a function of applied bias, transposed onto the 1.0 K experimental spectra of [1]. The relevant dot states all have the same $n_2 (= 1)$ quantum number ($n_2 = 2$ dot states are virtual), which is hereafter suppressed. There is general agreement between the experimental and predicted peak voltage

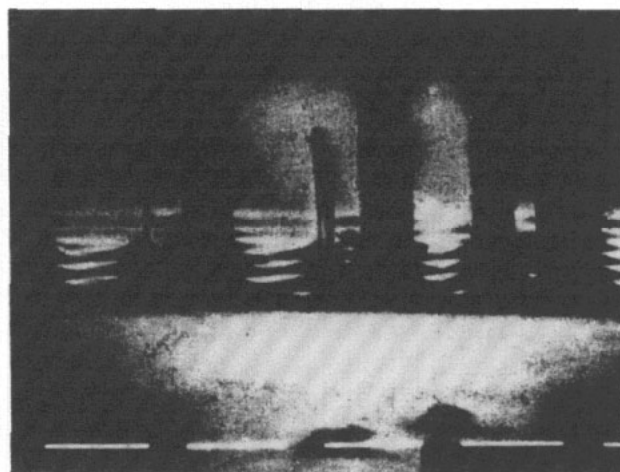


Figure 1. Scanning electron micrograph of an array of anisotropically etched columns containing a quantum dot. The horizontal white marker is 0.5 μm .

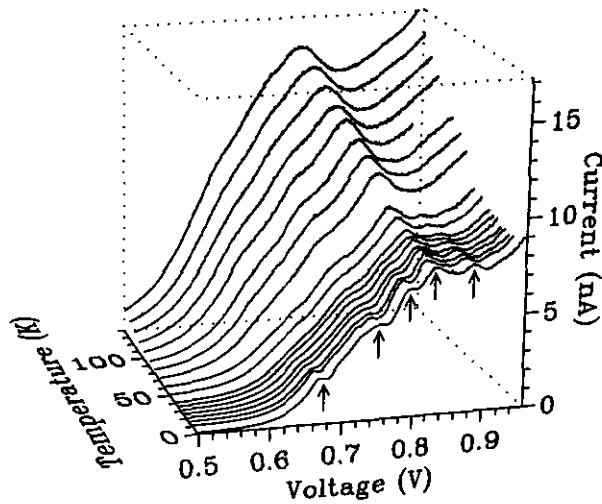


Figure 2. Current–voltage characteristics of the 1000 Å single-quantum-dot nanostructure [1] as a function of temperature, indicating resonant tunnelling through the discrete states of the quantum dot. The arrows indicate peak positions for the $T=1.0$ K curve.

positions. The $3'-3$ transition is not seen since the dot states become virtual at ~ 0.95 V. The 1D DOS in the emitter becomes thermally smeared when $3k_B T > \Delta E$ (the emitter subband spacing), and thus at high temperatures the only surviving transition is the $1'-1$. This indeed occurs when $3k_B T \sim 21$ meV, in good agreement with the subband spacing of 25 meV.

The observation of the momentum-non-conserving transitions (n' not equal to n) shows that k_{\perp} is not a good quantum number in this system, due to the hourglass topography of the electron energy surface. This absence of an n, n' (radial) selection rule is natural from the radially changing, cylindrically symmetric geometry that breaks translational symmetry.

3. 0D–0D tunnelling

An intriguing situation would be to examine the case of 0D–0D tunnelling, compared with the 1D–0D situation. The fabrication of such structures is relatively straight-

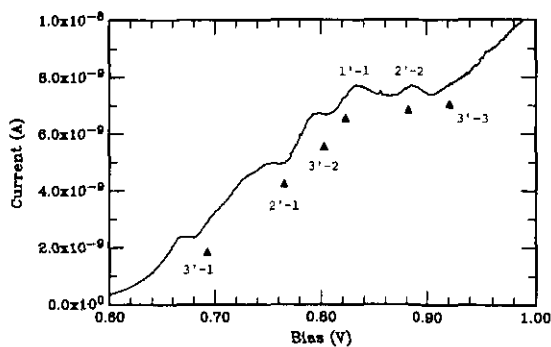


Figure 3. The crossings of the emitter subband level (n') with the quantum dot levels (n) as a function of applied bias, transposed onto the 1.0 K experimental spectra of figure 2.

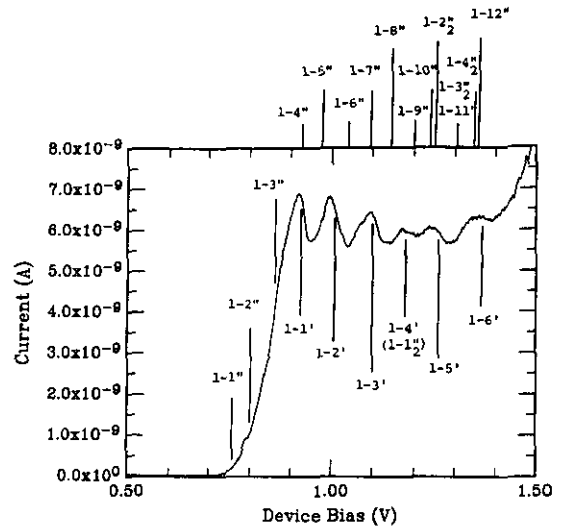


Figure 4. Current–voltage characteristic at $T=4.2$ K of the '0D–0D' sample, with predicted resonant peak positions superimposed. The notation is 1 (emitter subband)–(final state), for either the first (n') or second (n'') dot. The subscript (i.e., n_2'') denotes the $n_x=2$ excited state.

forward, using a double-well–triple-barrier initial epitaxial structure. The structure was designed so that state overlap was small (with respect to the lateral splitting energy), so that the 1D–0D and 0D–0D transitions could be compared. Lateral fabrication is similar to before.

Figure 4 shows the 4.2 K current–voltage characteristics of this structure. A similar modelling of the state crossings as described above was performed, and the spectra of the transitions are superimposed on the figure. The notation used here is 1 (emitter subband)–(final state), for either the first (n') or second (n'') (i.e., further downstream from the emitter) dot.

The spectra are well fitted by resonances occurring for crossings of the 0D states with the lowest 1D subband in the contact. The agreement is good for the major $(1-n')$ resonances, which are significantly stronger than the n'' states due to the thinner tunnel barrier. The position of the minor second set, $1-n''$, predicts the structure below the $1-1'$ peak. The peaks are not apparent at higher voltages, probably due to overlap with the $1-n'$ resonances.

The predicted 0D–0D crossing spectra give bad agreement both qualitatively (spacings and number of peaks) and quantitatively (peak positions); the predicted spacing of 0D–0D crossings are approximately 5 mV throughout the region examined. However, since the lateral potential of the adjacent dots is nearly identical, k_{\perp} is a good quantum number in the 0D–0D transitions, compared with the dramatic lateral potential variation in the 1D–0D transitions. Thus, the 0D–0D transitions would only occur for $n' = n''$, which is not experimentally accessible in this structure. Thus, we only observe the 1D–0D transitions (each separately), and not the 0D–0D transitions (the selection rule holds for $n' = n''$, and not for $n = n', n''$) since the lateral potential changes from the contact-to-dot region, but not for the dot-to-dot region.

4. Fermi level effect

It has been predicted [9] that 0D states will also contribute to resonances in the observed characteristics of dot tunnelling, when the 0D states under bias pass below the Fermi level. However, the observed structure of the resonances may be different from that when the 0D states pass below the 1D states, since there is a discontinuity in the density of states in this case.

Figure 5 shows the current–voltage and derivative–voltage characteristics of a structure where the separation of the quantum states is sufficiently small, and where the resonances can be observed at sufficiently low

bias, for this effect to be observed. When the first 0D state passes into the Fermi level, a step in current (peak in conductance) is observed; at higher bias, when this state passes through the minimum of the 1D emitter state, a NDR region is observed.

5. Summary

These structures provide a suitable system in which to explore quantum-confined electronic states, transitions, and selection rules involving those states. The epitaxial design freedom allows highly complex electronic state structures to be examined.

Acknowledgments

We are indebted to our collaborators W R Frensley, R J Aggarwal, Y-C Kao, R J Matyi, T M Moore, and A E Wetsel. We thank R T Bate for constant encouragement and support, and R K Aldert, E D Pijan, D A Schultz, D L Smith, P F Stickney and J R Thomason for technical assistance. This work was sponsored in part by ONR, ARO and WRDC.

References

- [1] Reed M A *et al* 1988 *Phys. Rev. Lett.* **60** 535
- [2] Reed M A *et al* 1989 *Advances in Solid State Physics (Festkörperprobleme)* vol 29, ed U Rossler (Braunschweig: Vieweg) pp 267–83
- [3] Tarucha S *et al* 1990 *Phys. Rev. B* **41** 5459; 1991 *Appl. Phys. Lett.* **58** 1623
- [4] Faini G *et al* 1991 *Resonant Tunneling in Semiconductors: Physics and Applications* ed L L Chang, E E Mendez and C Tejedor (New York: Plenum)
- [5] Su B *et al* 1991 *Appl. Phys. Lett.* **58** 747
- [6] Tewordt M *et al* 1990 *J. Phys.: Condens. Matter* **2** 8969
- [7] Dellow M W *et al* 1991 *Electron. Lett.* **27** 134
- [8] Groshev A 1990 *Proc. 20th Int. Conf. on Physics of Semiconductors* ed E M Anastassakis and J D Joannopoulos (Singapore: World Scientific) p 1238
- [9] Bryant G 1991 *Phys. Rev. B* **44** 3782

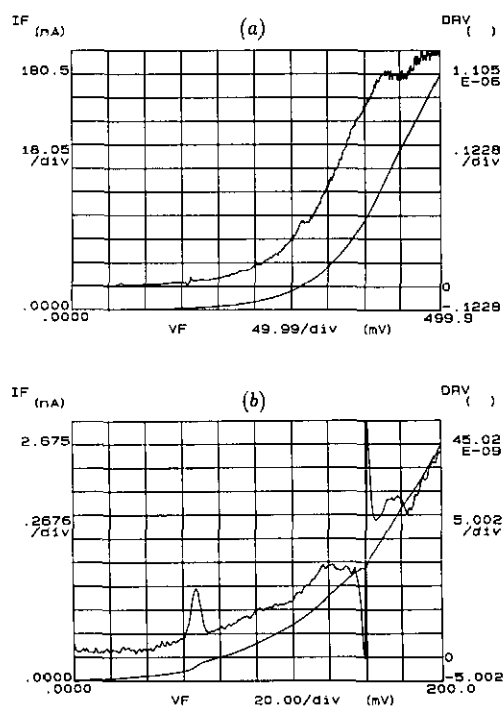


Figure 5. (a) Current–voltage and derivative–voltage characteristics at $T=4.2\text{ K}$ of an $\sim 1000\text{ \AA}$ quantum dot structure, illustrating the step in the current when the 0D state enters the Fermi level. (b) Expanded view of (a).